Vegetable Oil-based Hybrid Submicron Particles Loaded with JMV5038: A Promising Formulation against Melanoma

Koceïla Doufène, Yohan Malki, Laure-Anaïs Vincent, Pierre Cuq, Jean-Marie Devoisselle, Nicolas Masurier, Anne Aubert-Pouëssel

Version of Record: https://www.sciencedirect.com/science/article/pii/S0022354920306110
Manuscript_f01fd61c948dea638fa75378a2afe93d

Vegetable Oil-based Hybrid Submicron Particles Loaded with JMV5038:

A Promising Formulation against Melanoma

*Koceïla Doufène [1], Yohan Malki [2], Laure-Anaïs Vincent [2], Pierre Cuq [2], Jean-Marie Devoisselle [1], Nicolas Masurier [2] and Anne Aubert-Pouëssel [1]**

1 : Institut Charles Gerhardt Montpellier (ICGM), Univ. Montpellier, CNRS, ENSCM, Montpellier, France.

2 : Institut des Biomolécules Max Mousseron (IBMM), Univ. Montpellier, CNRS, ENSCM, Montpellier, France.

* : Email Address: anne.aubert@umontpellier.fr

Abstract

The aim of this work was to carry out a preformulation study on JMV5038 as a new potent cytotoxic agent, and to develop its formulation within vegetable oil-based hybrid submicron particles (HNP) in order to obtain a versatile dosage form against melanoma. JMV5038 was first characterized through physico-chemical tests and it exhibited high melting point and logP value, an important pH-sensitivity that led to the formation of well-identified degradation products at low pH, as well as a substantial solubility value in silylated castor oil (ICO). Then, JMV5038-loaded HNP were formulated through a thermostabilized emulsion process based on the sol-gel cross-linking of ICO. They showed high loading efficiency and their *in vitro* release kinetic assessed in a biorelevant PBS/octanol biphasic system showed a constant sustained release over one month. The cytotoxic activity and cytocompatibility of HNP were evaluated on A375 melanoma cells and NIH 3T3 cells, respectively. JMV5038-loaded HNP exhibited a slightly enhanced cytotoxic activity of JMV5038 on melanoma cells while demonstrating their safety on NIH 3T3 cells. In conclusion, JMV5038-loaded HNP proved to be an efficient and safe drug subcutaneous delivery system that will be interesting to evaluate through preclinical studies.

Abbreviations

API: Active Pharmaceutical Ingredient = drug

COSY: COrrelation SpectroscopY

HMBC: Heteronuclear Multiple Bond Correlation

HNP: Hybrid submicroN Particles

HPLC: High Pressure Liquid Chromatography

ICO: silylated Castor Oil

IP: ImidazoPyridine

IPTES: (3-IsocyanatoPropyl)TriEthoxysilane

MAPK/ERK: Mitogen-Activated Protein Kinases/Extracellular signal-Regulated Kinases

MWCO: Molecular Weight Cut-Off

NMR: Nuclear Magnetic Resonance

ORALD: Open-Ring and Alanine-Loss Derivative (of JMV5038)

ORD: Open-Ring Derivative (of JMV5038)

PBS: Phosphate Buffer Saline

RT: Retention Time

SD: Standard Deviation

UPLC (/ MS): Ultra Performance Liquid Chromatography (Coupled with Mass Spectrometry)

1. Introduction

Skin cancer is one of the most common cancers in the world with an incidence of 2 ‰,[1] and it is one of the most expanding over the last decades with continuously increasing cases mainly due to sunlight repeated exposures and to changes in the thickness of the ozone protective layer.[2] Melanoma represents 10 % of the skin cancers, and is by far the deadliest form in the world (60,000 deaths per year) affecting young adults with an average age of 35 years.[3] Indeed, the resistance of melanoma cells to pharmacological treatment constitutes a critical issue on the way of anti-cancer therapy. Various oncogenic mutations were found in 90 % of cutaneous melanomas,[4] mainly the activating BRAF mutation (50 % of melanomas). In fact, BRAF is a serine / threonine protein kinase involved in several mechanisms underlying melanomagenesis. Most of these mechanisms are triggered by the deregulated activation of the downstream MAPK / ERK signaling pathway which promote cell proliferation and migration.[5] Research carried out on these mechanisms has made it possible to adapt treatments according to the mutations detected.[6]

Melanoma treatment protocols are based on surgery, chemotherapy and immunotherapy. For over 20 years, dacarbazine was the only chemotherapeutic treatment approved by the US Food and Drug Administration but recently, breakthroughs have been made in the areas of monoclonal antibody immunotherapies and MAPK pathway-targeted therapies (e.g., vemurafenib and dabrafenib).[7] Despite these innovations, there are still non-responder patients, and the rapid emergence of drug resistance to initially responsive cancers has globally led to only marginal patient benefit.[8] Numerous treatment options emerged over the past decade, most of them aimed to increase efficiency and reduce side effects through therapeutic combination approaches. Other strategies leveraging advances in nanotechnology provided the same benefits.[9] Indeed, various nanoparticles were considered either as anti-melanoma agents (e.g., carbon nanotubes, copper and gold nanoparticles) or as drug carriers of anti-melanoma molecules (e.g., lipid nanoparticles, liposomes, nanomemulsions), and they permitted the administration via several routes (e.g., intravenous, intralesional, oral, topical).

In previous studies, we developed new imidazopyridine-fused [1,3]-diazepinones molecules and highlighted their potential as cytotoxic agents against several cancer cell lines, including several melanoma cell lines.[10–12] The hit of this family, referred to as JMV5038, showed a high efficiency on melanoma cells and no toxicity on fibroblast cells (IC_{50} > 100 µM).[12] However, and like most active pharmaceutical ingredients (APIs) in the pipeline,[13] JMV5038 exhibited a poor aqueous solubility

(7.75 µg·ml^{-1} in PBS) and the formulations tested so far, based on the classical use of hydrophilic surfactants or co-solvents for parenteral administration (data not shown here), have failed.

A common strategy applied in the formulation of poorly water-soluble APIs is the use of lipid-based drug delivery systems. Indeed, these systems have shown their high solubilizing capacities of poorly water-soluble APIs, and their suitability for parenteral administration. Hence, several forms are on the market (e.g. Diprivan®: a lipidic emulsion of propofol, Daunoxome®: a liposomal formulation of daunorubicin). Besides, innovative lipid-based drug delivery systems in anti-cancer therapies were developed and showed promising early results, such as nanoemulsions of paclitaxel[14] or solid lipid nanoparticles of doxorubicin, idarubicin,[15] paclitaxel[16] and camptothecin.[17] However, these systems often exhibit a limited stability and low loading capacity of very lipophilic APIs, and only few studies were conducted to develop appropriate alternatives.[18,19] In order to meet these requirements, we propose here an original hybrid drug delivery system that combines advantages of lipid-based systems and of silicon in order to develop a stable, efficient, and versatile dosage form of JMV5038. Indeed, lipid-based systems are well-known for their biocompatibility and their high solubilizing capacity of poorly water-soluble molecules, and silicon provides high structuring capacity as a mineral part of this hybrid system, while being biocompatible. Moreover, sol-gel crosslinking of the mineral part makes possible to obtain amorphous solid dispersions of high melting point molecules, and to stabilize the latter in high energy states.

Hybrid submicron particles (HNP) made of silylated castor oil (ICO) cross-linked by sol-gel chemistry were developed by means of a simple emulsification process in order to entrap JMV5038 while maintaining its biological activity. First of all, a preformulation study was performed to characterize JMV5038 prior to the selection of its optimal formulation. Suitable conditions were required to prevent the degradation of JMV5038, whereas the degradation products were thoroughly identified in order to set-up a quality procedure. Then, pharmacotechnical tests were conducted to show in particular the ability of HNP to efficiently entrap and to release JMV5038. Finally, *in vitro* cellular tests were performed to quantify the cytotoxic activity of the released JMV5038 on A375 human melanoma cells, and to underline the cytocompatibility of the developed formulation on NIH 3T3 non cancer cells.

2. Material and methods

2.1. Material

Pharmaceutical grade castor oil (Mw = 934 g·mol^{-1}) was purchased from Cooper Pharmaceutique. (3-Isocyanatopropyl)triethoxysilane (IPTES; Mw = 247.3 g·mol^{-1}), κ-carrageenan, solvents and reactants (acetonitrile, 4-bromobenzoic acid, dichloromethane, 1-Ethyl-3-(3-dimethylaminopropyl)carbodiimide hydrochloride, hydroxybenzotriazole, methanol, octanol and triethylamine) were supplied by Sigma-Aldrich.

A375 human melanoma cancer cell line aimed to the cytotoxic activity assays, and NIH 3T3 fibroblast cell line aimed to the cytocompatibility assays, were both obtained from ATCC.

2.2. Synthesis of JMV5038 and of its open-ring derivative (ORD)

JMV5038 (Fig. 1) was synthesized according to our previous reported procedure, and its physical characteristics were in agreement with the published data (purity > 99 %, Mw = 369 g·mol^{-1}) [20].

Preliminary tests (not shown here) have demonstrated the sensitivity of JMV5038 to a formulation in an acidic medium. In order to check the assumption of diazepine ring opening when JMV5038 is formulated in these conditions, the open-ring derivative (ORD ; Fig. 1) of JMV5038 was synthesized as follows: to a solution of (2*S*)-2-amino-1-(2-aminoimidazo[1,2-*a*]pyridin-3-yl)-propan-1-one[20] (471 mg, 2.31 mmol) in dichloromethane (50 ml) at 0°C, were added hydroxybenzotriazole (346 mg, 2.54 mmol, 1.1 equiv.), 1-ethyl-3-(3-dimethylaminopropyl)carbodiimide hydrochloride (487 mg, 2.54 mmol, 1.1 equiv.), triethylamine (353 µl, 2.54 mmol, 1.1 equiv.), and 4-bromobenzoic acid (201 mg, 2.54 mmol, 1.1 equiv.). The resulting mixture was stirred at 0°C for 30 min and then at room temperature for 6 h. After completion of the reaction (monitoring by thin-layer chromatography), the solution was washed with saturated $NaHCO_3$ aqueous solution (3 x 30 ml). The organic layers were combined, dried over Na_2SO_4, filtered and the solvent was removed under reduced pressure. The residue was dissolved in dichloromethane and filtered through alumina gel using sintered glass Büchner funnel. The solvent was removed in vacuo to afford the ORD as a white solid (417 mg, 47 % yield, > 95 % purity); mp: 110 – 111 °C; $[\alpha]_D^{20}$ = +4.8 ° (*c* 1.0, $CHCl_3$); ^{1}H NMR (DMSO d_6, 500 MHz): δ ppm 1.43 (d, 3H, *J* = 6.9 Hz), 5.24 (q, 1H, *J* = 7.1 Hz), 6.73 (bd s, 2H), 6.97 (td, 1H, *J* = 1.3 Hz, *J* = 6.9 Hz), 7.36 (dt, 1H, *J* = 1.0 Hz, J = 8.8 Hz), 7.50 (td, 1H, *J* = 1.4 Hz, J = 7.1 Hz), 7.69 (d, 2H, *J* = 8.6 Hz), 7.89 (d, 2H, *J* = 8.6 Hz), 9.01 (d, 1H, *J* = 7.2 Hz); ^{13}C NMR (DMSO d_6, 100 MHz): δ ppm 17.4, 51.0, 113.0, 114.1, 125.7, 129.0,

130.2, 130.8, 131.7, 133.2, 147.5, 166.2, 185.7; HPLC, RT = 1.07 min; MS (ESI+): m/z 387.1 $[M+H]^+$, 389.1 $[M+H+2]^+$; HRMS calcd for $C_{17}H_{16}BrN_4O_2$ 387.0457, found 387.0451.

(Fig. 1)

2.3. Preformulation study of JMV5038

The determination of the melting point, the solubility, and the lipophilicity of an active pharmaceutical ingredient are key steps to choose its appropriate formulation.[21] In order to study the thermal behavior of JMV5038, a thermogravimetric analysis (STA 6000, PerkinElmer) and a differential scanning calorimetry (DSC4000, PerkinElmer) were carried out. During the first, 10 mg of JMV5038 were heated from 25 to 600 °C and during the second, 5 mg of JMV5038 in a hermetically sealed aluminum pan were heated from 25 to 200 °C. Both analyses were conducted at 5 °C·min^{-1} rate under nitrogen flow. Besides, the thermal behavior of ORD was studied in the same conditions. For determination of the JMV5038 lipophilicity, the XLOGP3 algorithm was requested.[22]

The solubility of JMV5038 in ICO was measured as follows: 15 mg (40.65 µmol) of JMV5038 were put into 285 mg of ICO (i.e. 5 wt.% saturated mixture), then the mixture was gently stirred during 24 h at room temperature. After that, the mixture was centrifuged at 12000 rpm during 30 min, and 50 mg of the supernatant were diluted 200 times in methanol. The obtained solution was analyzed by HPLC (integration at λ =214 nm). The system consisted of a Beckman System Gold HPLC, using a Merck Chromolith® SpeedROD C18, 25 x 4.6 mm reversed-phase column. A flow rate of 3 ml·min^{-1} and a gradient of (0–100) % B over 5 min were used (eluent A: water / 0.1 % CF_3CO_2H; eluent B: acetonitrile / 0.1 % CF_3CO_2H). Quantitative determination was obtained by mean of a calibration curve (r^2 = 0.9923); standards were diluted in methanol within a concentration range of 0 up to 1500 µM.

2.4. Formulation of unloaded and JMV5038-loaded hybrid submicron particles

The silylation of castor oil to obtain ICO was detailed elsewhere.[23] Herein, ICO 0.8 was used, meaning that 80 % of hydroxyl groups of the castor oil were grafted with isocyanate groups of (3-Isocyanatopropyl)triethoxysilane.

Unloaded and JMV5038-loaded HNP were formulated following a thermostabilized oil-in-water emulsification process combined with sol-gel crosslinking. The outlines of the formulation method were described in a previous study [23], but has been adapted here to constraints of submicron sizing and of

soft processing related to the pH-sensitivity of JMV5038. For the formulation of JMV5038-loaded HNP, a preliminary step of JMV5038 dissolution in ICO 0.8 (2 wt.%) was required. The ICO 0.8 ± JMV5038 was emulsified in an acidic (acetate aqueous buffer, pH = 2.7) or neutral (milli-Q water, pH = 6.5) aqueous medium containing 0.5 wt.% carrageenan at 60 °C, using an ultrasonic probe (Branson® Sonifier 250 equipped with a 3 mm tapered microtip) to obtain submicron droplets. A fast cooling down to 4 °C allowed to "freeze" the aqueous continuous phase by means of the dissolved carrageenan, and thus to immobilize the nanodroplets of unloaded or JMV5038-loaded ICO 0.8. After that, the sol-gel crosslinking occurred inside the nanodroplets during 10 days at room temperature and led to the formation of unloaded or JMV5038-loaded HNP. After washing, HNP were resuspended in PBS (150 mM, pH = 7.4).

After synthesis, the HNP were observed under optical microscopy (EVOS® FL Imaging System, Thermo Fisher Scientific) and their size was measured by dynamic light scattering (Zetasizer Nano ZS®, Malvern Panalytical). The loading efficiency was assessed by extracting JMV5038 from HNP in octanol over 24 h, prior to an UPLC / MS analysis by a Waters Acquity H-Class Plus®, coupled to a Waters SQD2 spectrometer® (electrospray ionization mode, ESI+). All the analyses were carried out using an analytic C18 reversed-phase column (Acquity UPLC® BEH C18, 1.7 µm, 50 x 4.6 mm, Waters®). A flow rate of 0.6 ml·min^{-1} and a gradient of (0–100) % B over 5 min were used (eluent A: water / 0.1 % HCO_2H; eluent B: acetonitrile / 0.1 % HCO_2H). Nitrogen was used for both the nebulizing and drying gas. The data were obtained in a scan mode ranging from 100 to 1000 m/z in 0.1 s intervals; 10 scans were summed up to get the final spectrum. The chromatograms of the extracts from JMV5038-loaded HNP formulated in acidic and neutral media were then compared to the JMV5038 and ORD chromatograms as references. The identity of the compounds was confirmed by mass spectrometry.

2.5. *In vitro* release tests of JMV5038 from hybrid submicron particles

Release tests of JMV5038 from HNP have been carried out in a PBS/octanol biphasic system, which was selected as a biorelevant system that mimics the *in vivo* conditions of API release (Fig. 2) as reported for several other systems [24–26]. Our system was composed of a dialysis device (MWCO = 12 kDa) that contains 3 ml of JMV5038-loaded HNP suspension, immersed in 100 ml PBS (pH = 7.4, T = 37 °C, rotation = 100 rpm) as a physiological simulated phase, and 10 ml of octanol as a storage phase that entrap the JMV5038 released from the HNP. 500 µl samples of the upper phase were

collected at determined times prior to an UPLC / MS dosage (conditions detailed above), and 500 µl of fresh octanol were added after each sampling to maintain the volume constant. Finally, a percentage curve of JMV5038 released over time was drawn for a triplicate.

(Fig. 2)

2.6. *In vitro* activity assays

The A375 human melanoma cells were cultured in Dulbecco's Modified Eagle Medium (DMEM, Sigma Aldrich) supplemented with 10 % heat-inactivated foetal calf serum (FCS, Gibco), 2 mM Glutamax® (Gibco), 100 IU·ml^{-1} penicillin G sodium (Sigma Aldrich), 100 IU·ml^{-1} streptomycin sulfate (Sigma Aldrich). The cells were allowed to grow at 37 °C in a fully humidified atmosphere containing 5 % CO_2. A viability assay was used to evaluate the cytotoxic activity on A375 melanoma cells as previously described.[12] Cells were seeded at a final concentration of 2000 cells per well in 96-well microtiter plates for 24 h. Then, cells were exposed to negative control (1 % PBS in culture medium for submicron particles or 1 % DMSO in culture medium for JMV5038 and for ORD), or to particles in suspension into PBS or to JMV5038 or ORD freshly dissolved in DMSO, in a range of concentration from 0.01 to 40 µM (six wells per concentration). After 72 h of incubation, cells were stained with new medium containing 50 µg·ml^{-1} of neutral red (3-amino-7-dimethylamino-2-methylphenazine hydrochloride, Sigma Aldrich) at 37 °C for 2 h. The neutral red medium solution was then removed and the wells were washed with PBS. Finally, 100 µl of solution containing ethanol, acetic acid and water (50/1/49 v/v/v respectively) were added into the wells and the absorbance was measured at 540 nm using the microplate reader 352 Multiscan MS (Labsystems). Cell survival rates were normalized to the absorbance values of untreated control cells. IC_{50} was obtained using a logistic regression model on Origin software, and the loading rate of JMV5038 within loaded HNP (i.e. 2 wt.%) was considered in order to relate the cell survival rates to four corresponding concentrations of HNP (from 8 up to 675 µg·ml^{-1}). Results are given as the mean ± standard deviation (SD) of three independent experiments, and statistical analysis was performed using the Student's t-test.

2.7. Cytocompatibility evaluation of unloaded and JMV5038-loaded hybrid submicron particles

Cytocompatibility direct assays were conducted according to the ISO 10993-5 standard. The NIH 3T3 cells were seeded to be 5000 per well into a 96-well culture dish plate containing 200 µl per well of culture medium (composition listed above) for 24 h. Simultaneously, unloaded and JMV5038-loaded HNP were suspended in culture medium, both at 1350 $\mu g \cdot ml^{-1}$ during 24 h. Subsequently, the cells were treated with the HNP suspensions diluted in the culture medium at several concentrations ranging from 1350 down to 8 $\mu g \cdot ml^{-1}$, or with a fresh culture medium for the negative control cells.

After 48 h of exposure, the viability of NIH 3T3 cells treated or not with unloaded and JMV5038-loaded HNP was measured using a CellTiter 96® AQ cell proliferation assay (Promega) composed of a tetrazolium compound (3-(4,5-dimethylthiazol-2-yl)-5-(3-carboxymethoxyphenyl)-2-(4-sulfophenyl)-2H-tetrazolium, inner salt; MTS) and an electron coupling reagent (phenazine methosulfate; PMS), as follows: 20 µl of a mixture MTS-PMS was added in each well for 3 h reaction with the cells, then the assay plate was read at 490 nm using a microplate reader (Multiskan Go, Thermo Fisher Scientific). Finally, cell viability rates were normalized to the absorbance values of the negative control cells (100 % viability). Results are given as the mean ± SD of three independent experiments and statistical analysis was performed using the Student's t-test.

3. Results and discussion

3.1. Physicochemical characterization of JMV5038 and ORD

Thermal gravimetric analyses of JMV5038 and its ORD are depicted in Fig. 3. A loss of 4 % weight was observed for both compounds between 90 and 120 °C, probably due to an evaporation of hygroscopic water. For JMV5038, a slight loss was recorded after 190 °C highlighting the onset of degradation, followed by a massive loss after 270 °C. The residual mass at 600 °C was 40.2 % of the initial JMV5038 mass, and was consistent with previous studies performed on imidazopyridine (IP) derivatives.[27] Regarding to the ORD, earlier onsets of degradation (i.e. 140 °C) and of massive weight loss (i.e. 240 °C) as well as a lower residual mass (i.e. 28.6 % of the initial ORD mass) were observed. Hence, the better thermostability of JMV5038 compared to its ORD underlines the key role held by the diazepine central ring for the structural stability of these compounds.

The differential scanning calorimetry analysis (Fig. 4) showed an endothermic peak at 166 °C assigned to the fusion of JMV5038 crystals, followed by an exothermic one at 192 °C that supports the TGA results (onset of JMV5038 degradation). Nevertheless, the ORD thermogram did not show any significant event in these conditions when we were expecting a fusion peak around 110 °C. The difference of energy needed for the state change appears to be very small, highlighting the presence of weak bonds between ORD molecules.

(Fig. 3 and 4)

The computed value of LogP (JMV5038) was 4.01, suggesting that the molecule is very lipophilic. Indeed, this value means that the partition coefficient of JMV5038 in octanol / water mixture is 10233 / 1, respectively. Overall, the preformulation tests revealed that JMV5038 has a significant hydrophobicity considering its high LogP, along with a strong crystalline binding energy evidenced by its high melting point. Thus, formulating JMV5038 within HNP is highly suitable since these particles combines the advantages of lipid-based drug delivery systems that should solubilize the hydrophobic JMV5038, and of amorphous solid dispersions that should break the crystalline bonds.

The solubility of JMV5038 in ICO 0.8 was measured to be 34 ± 1 $mg \cdot ml^{-1}$ (i.e. 3.4 wt.%, corresponding to 92 ± 3 mM), meaning that JMV5038 is nearly 4400 times more soluble in ICO 0.8 than in PBS. Hence, this high solubility result concludes the preformulation study and makes possible a further formulation of JMV5038 in HNP.

3.2. Formulation of the hybrid submicron particles

In contrast to the mechanical stirring we used in a previous study,[23] the ultrasonic emulsification process allowed to decrease the droplet size down to submicron either in acidic or neutral medium. The resulting HNP showed a reasonably homogeneous size centered on 615 nm allowing their administration through several routes, as discussed hereafter. They were solid, spherical, well-isolated, and they exhibited a smooth surface on optical microscopy (Fig. 5), with both formulation protocols.

(Fig. 5)

Furthermore, the loading efficiencies of JMV5038 in HNP were substantially different according to the pH of the formulation medium. Indeed, HNP formulated in neutral medium showed a loading efficiency of 80 ± 1 %, corresponding to an effective loading rate of 397 ± 3 $\mu g \cdot ml^{-1}$ in the HNP suspension (i.e. 1.076 mM) whereas those formulated in acidic medium entrapped less than 1 % of JMV5038 and revealed also a partial degradation of JMV5038 through UPLC / MS analysis (chromatogram A in Fig. 6).

(Fig. 6)

Three main peaks were found in chromatogram A. The peak at 1.94 min corresponded to JMV5038 (same retention time and mass spectrum than pure JMV5038, chromatogram D). The compound at 2.60 min showed an increase of mass of 18 Da compared to JMV5038 and corresponded to the ORD that we synthesized (same retention time and mass spectrum than pure ORD, chromatogram C). Its formation was attributed to the opening of the diazepine ring due to acidic conditions used in the formulation (Scheme 1, way A). Another compound, among other minor ones, was also formed (retention time at 2.32 min). Its mass pattern confirmed the presence of a bromine atom in its structure (molecular ions at 316 and 318 Da) indicating that this compound is also derived from JMV5038, but with a loss of one part of the molecule. This compound was separated from the crude by preparative HPLC and then analyzed by NMR. The analysis of the ^{1}H and the ^{1}H-^{1}H COSY spectra indicated the presence of a *para*-substituted phenyl group and four aromatic protons, which were attributed to the protons of the pyridine nucleus. Furthermore, the presence of a singulet at 8.31 ppm and another one at 11.5 ppm was attributed to the apparition of one proton in the IP nucleus (position “b”) and to a NH of an amidic function, respectively. A ^{1}H-^{13}C HMBC analysis revealed a correlation between the singulet at 8.31 ppm and the carbone “c” of the IP nucleus, confirming the structure of this compound. A possible mechanism to explain the formation of these two compounds of degradation in acidic medium is shown in Scheme 1. Protonation of the nitrogen “a” of the diazepine ring, followed by hydrolysis could lead to the opening of the diazepine ring and the formation of ORD (way A). Alternatively, the IP ring could react at position “b” with a proton (way B). Indeed, IP derivatives are known to be sensitive to electrophilic aromatic substitutions, and this position is the most preferred position for these reactions.[28] Then, the carbonyl group could be attacked by a water molecule to lead

to the opening of the diazepine ring. Then, as previously described for ORD, imine protonation followed by its hydrolysis and loss of one molecule of alanine could lead to the formation of ORALD (Open-Ring and Alanine-Loss Derivative).

Finally, the analysis of the payload from HNP formulated in neutral medium did not show these compounds of degradation (chromatogram B in Fig. 6). Hence, the formulation process in neutral medium has been retained for all the subsequent tests.

(Scheme 1)

3.3. *In vitro* release tests on JMV5038-loaded hybrid submicron particles

(Fig. 7)

The release kinetic of JMV5038 from HNP (Fig. 7) exhibited a sustained, constant and complete release profile over 28 days, underlining the potential of HNP as a long-acting drug delivery system. No burst effect was pointed out (10 ± 3 % released after 24 h) attesting that JMV5038 was entrapped within the HNP matrix, and was not adsorbed on the surface. It may be noted that this release profile differs from the one obtained in a previous study we conducted on micrometer-sized hybrid particles loaded with ibuprofen,[23] which showed a double stage release with a burst effect (26 ± 3 % of ibuprofen released after 24 h). In fact, we were expecting a faster release with HNP because of their higher surface area, but it seems that the physicochemical nature of the API is more determinant in the release profiles. Indeed, JMV5038 has a higher molecular weight (369 $g \cdot mol^{-1}$), a higher melting point (166 °C), and no labile proton compared to ibuprofen (206 $g \cdot mol^{-1}$, 76 °C, and one carboxylic proton respectively).

The sustained constant release profile along with the submicron size of HNP allow several routes of administration. For example, the subcutaneous injection of the HNP suspension can be considered since the critical criteria were fulfilled.[29] Indeed, the volume of each sample used during the release tests was 3 ml according to the maximum subcutaneously tolerated volume, and the release rate was constant with an average of 115.6 nmol per 24 h corresponding to 3.6 % of the entire payload. The HNP suspension is also suitable for intratumoral administration ensuring *in situ* cytotoxic activity on the

cancer cells, when the tumor removal is not possible. An original approach already described[30] would be the cutaneous deposition by holding the HNP on the surface of the lesion in a wound dressing. However, these assumptions have to be confirmed in future preclinical studies.

Finally, the intravenous administration could be considered by further reducing the HNP size in order to allow them reaching the tumor sites through passive or active targeting. Passive targeting of melanoma cells can be achieved by the enhanced permeability and retention (EPR) effect that allows accumulation of the circulating nanosized drug delivery system in tumors much more than they do in healthy tissues[31]. The EPR effect was already pointed out with liposomes and nanoparticles (e.g., nanoparticle formulation of paclitaxel[32]), and is mainly permitted by their specific nanometric size lower than 150 nm. Moreover, the PEGylation (i.e. grafting of poly(ethylene glycol) chains on the surface) of our nanosized drug delivery system would be a complementary approach leading to a prevention from a capture by the mononuclear phagocyte and reticuloendothelial systems, and to an increase of its uptake by the cancer cells (e.g., PEGylated liposomal formulation of doxorubicin[33]). Active targeting may also be considered in melanoma treatment by anchoring specific antibodies on the surface of JMV5038-loaded HNP when the corresponding antigen is expressed on the cancer cells (e.g., anti αvβ3 integrin antibodies anchored on doxorubicin-loaded human serum albumin nanoparticles[34]).

3.4. *In vitro* activity assays

(Fig. 8)

First, we evaluated the cytotoxic activity profile of unloaded HNP in A375 melanoma cells, using neutral red uptake viability assay. We observed that, even at 675 $\mu g \cdot ml^{-1}$ over a period of 72 h, cell viability was not significantly reduced, compared to the control experiments (Fig. 8A). This result indicates that such unloaded particles have no toxic effect on the cells. The *in vitro* anticancer activity of JMV5038-loaded HNP was then evaluated in A375 cells at different concentrations through 72 h of incubation. At 8.33 $\mu g \cdot ml^{-1}$ of loaded HNP, only a weak cytotoxicity was observed, probably due to a too low concentration of the released free API (Fig. 8A). Indeed, if 100 % of API release from the HNP is assumed, the concentration of JMV5038 was about 0.45 µM, which was about 4.5 times less than the IC_{50} of JMV5038 (IC_{50} = 2.10 ± 0.42 µM).[12] If 20 % of release is considered as demonstrated above during *in vitro* release tests (Fig. 7), the concentration fell to 0.09 µM, which was about 23 times less

than the IC_{50} of the free API. At higher concentrations of JMV5038-loaded HNP (75 to 675 µg·ml^{-1}), cell viability decreased dramatically, proving that the formulation process in neutral medium did not alter the biological activity of JMV5038 (Fig. 8A and 8B). Considering 20 % of drug release after 72 h, the IC_{50} of JMV5038-loaded HNP was determined to be 1.58 ± 0.03 µM (Fig. 8C). This value, slightly lower than that of the free API, could be explained by a better ability of the HNP to penetrate into the cells and deliver the API compared to free JMV5038. The ORD, corresponding to an opening of the diazepine ring that occurs when loaded HNP are formulated in an acidic medium, was totally inactive (IC_{50} > 40 µM, Fig. 8C). Thus, the process developed here to formulate JMV5038-loaded HNP in neutral medium was able to ensure the integrity of the API and to maintain its biological activity.

3.5. Cytocompatibility assays

(Fig. 9)

In order to contrast the activity of JMV-loaded HNP on melanoma cells with their safety on healthy tissues, we performed cytocompatibility tests on NIH 3T3 cells in the same conditions and concentration range (Fig. 9). For the lowest concentrations of unloaded and loaded HNP (i.e. 8.33 and 75 µg·ml^{-1}) all the cells survived, but a slight decrease in viability started to appear at 225 µg·ml^{-1} (i.e. 88 ± 5 % and 84 ± 8 %, respectively). For higher concentrations of unloaded HNP (up to 1350 µg·ml^{-1} of particles), the viability stabilized at around 75 %, whereas for loaded HNP the cell viability decreased and stabilized until 58 ± 1 % for the highest concentration tested. Despite these very high concentrations, the IC_{50} was not reached, highlighting a low cytotoxicity. Overall, these results underline satisfying and quite similar cytocompatibility profiles of the unloaded and JMV5038-loaded HNP on NIH 3T3 fibroblasts, in line with the previous data we obtained using free JMV5038 (IC_{50} > 100 µM).[12]

A more detailed look brings out two further conclusions: first, at 675 µg·ml^{-1} of unloaded HNP, NIH 3T3 cells were more sensitive than A375 cells (viability of 75 ± 5 % compared to 95 ± 7 %). It suggests that the submicron particles (loaded or not) have a non-negligible effect at very high concentrations on cultured NIH 3T3 probably due to a disruption of *in vitro* cell growth that might not be found *in vivo*.

This effect was not observed with A375 melanoma cells because they are known to grow even under harsh conditions.

Secondly, the moderate cytotoxicity of loaded HNP highlighted a specificity of JMV5038 action according to the cellular type. Indeed, comparison with results obtained on melanoma cells (Fig. 8A) showed that when considering the toxicity onset of the loaded HNP (i.e. 8.33 $\mu g \cdot ml^{-1}$ on A375 vs. 225 $\mu g \cdot ml^{-1}$ on NIH 3T3), it appears that their minimum activity threshold is 27 times lower on the melanoma cells than on the fibroblasts. When considering the active concentrations on melanoma cells (i.e. 75 $\mu g \cdot ml^{-1}$ and higher), it appears that around 50 % more NIH 3T3 cells survive compared to A375 cells for the same concentrations. Hence, we can easily assume that the formulation has an effective anti-melanoma activity, while ensuring a sufficient margin of safety when administered *in vivo* for further preclinical studies.

4. Conclusion

In this paper, we covered two complementary studies aiming to the development of an efficient and versatile dosage form of JMV5038 as a new potent cytotoxic agent we previously developed against melanoma.

First, the preformulation study conducted on JMV5038 highlighted its high lipophilicity and its strong crystalline binding energy, along with its interesting solubility in ICO. The latter outcome opened the way for the second study that consisted in the development of a stable and efficient formulation of JMV5038 in HNP. The thermostabilized emulsion process we usually perform to formulate hybrid particles was adjusted here according to the pH-sensitivity of JMV5038, and to the particle size reduction we intended. HNP of homogeneous size and of high loading efficiency were thus obtained, allowing intratumoral, topical, as well as subcutaneous administration. The *in vitro* release kinetics of JMV5038 from HNP in a biorelevant PBS/octanol biphasic system showed a constant and sustained release profile (3.6 % of the entire payload per day, over 28 days), underlining the potential of HNP as a long-acting system of JMV5038 delivery. On the other hand, *in vitro* assays conducted on A375 melanoma cell line highlighted an enhanced activity of JMV5038 when formulated in HNP compared to the free JMV5038, contrasting with satisfying outcomes of cytocompatibility obtained on NIH 3T3 cells.

In sum, the JMV5038-loaded HNP proved to be efficient against melanoma and the preliminary outcomes brought out a sufficient safety of the formulation for further development through preclinical studies.

Acknowledgments

Authors thank the Algerian government for the Ph.D grant to Koceïla Doufène and the Franco-Algerian steering committee for its support. The authors are willing to thank Pierre Sanchez for UPLC / MS analyses, and Jean-Jacques Robin for its scientific advice on thermal analysis. This work was partially funded through ANR (the French National Research Agency) under the "Investissements d'avenir" programme with the reference ANR-16-IDEX-0006.

References

1. Khazaei Z, Ghorat F, Jarrahi AM, Adineh HA, Sohrabivafa M, Goodarzi E. Global incidence and mortality of skin cancer by histological subtype and its relationship with the human development index (HDI); an ecology study in 2018. *World Cancer Res J*. 2019;6(April 2019). doi:10.32113/wcrj_20194_1265

2. World Health Organization. *Skin Cancers*. https://www.who.int/uv/faq/skincancer/en/index1.html

3. Karimkhani C, Green AC, Nijsten T, et al. The global burden of melanoma: results from the Global Burden of Disease Study 2015. *Br J Dermatol*. 2017;177(1):134-140. doi:10.1111/bjd.15510

4. Najem A, Krayem M, Perdrix A, et al. New Drug Combination Strategies in Melanoma: Current Status and Future Directions. *Anticancer Res*. 2017;37(11):5941-5953.

5. Savoia P, Fava P, Casoni F, Cremona O. Targeting the ERK Signaling Pathway in Melanoma. *Int J Mol Sci*. 2019;20(6):1483. doi:10.3390/ijms20061483

6. Ascierto PA, Kirkwood JM, Grob J-J, et al. The role of BRAF V600 mutation in melanoma. *J Transl Med*. 2012;10(1):85. doi:10.1186/1479-5876-10-85

7. Luther C, Swami U, Zhang J, Milhem M, Zakharia Y. Advanced stage melanoma therapies: Detailing the present and exploring the future. *Crit Rev Oncol Hematol*. 2019;133:99-111. doi:10.1016/j.critrevonc.2018.11.002

8. Ambrosi L, Khan S, Carvajal RD, Yang J. Novel Targets for the Treatment of Melanoma. *Curr Oncol Rep*. 2019;21(11):97. doi:10.1007/s11912-019-0849-4

9. Mishra H, Mishra PK, Ekielski A, Jaggi M, Iqbal Z, Talegaonkar S. Melanoma treatment: from conventional to nanotechnology. *J Cancer Res Clin Oncol*. 2018;144(12):2283-2302. doi:10.1007/s00432-018-2726-1

10. Gallud A, Vaillant O, Maillard LT, et al. Imidazopyridine-fused [1,3]-diazepinones: Synthesis and antiproliferative activity. *Eur J Med Chem*. 2014;75:382-390. doi:10.1016/j.ejmech.2014.01.044

11. Bellet V, Lichon L, Arama DP, et al. Imidazopyridine-fused [1,3]-diazepinones part 2: Structure-activity relationships and antiproliferative activity against melanoma cells. *Eur J Med Chem*. 2017;125:1225-1234. doi:10.1016/j.ejmech.2016.11.023

12. Baccon-Sollier PL, Malki Y, Maye M, et al. Imidazopyridine-fused [1,3]diazepinones: modulations of positions 2 to 4 and their impacts on the anti-melanoma activity. *J Enzyme Inhib Med Chem*. 2020;35(1):935-949. doi:10.1080/14756366.2020.1748024

13. Bergström CAS, Porter CJH. Understanding the Challenge of Beyond-Rule-of-5 Compounds. *Adv Drug Deliv Rev*. 2016;101:1-5. doi:10.1016/j.addr.2016.05.016

14. Ye J, Dong W, Yang Y, et al. Vitamin E-rich Nanoemulsion Enhances the Antitumor Efficacy of Low-Dose Paclitaxel by Driving Th1 Immune Response. *Pharm Res*. 2017;34(6):1244-1254. doi:10.1007/s11095-017-2141-3

15. Cavalli R, Caputo O, Gasco MR. Solid lipospheres of doxorubicin and idarubicin. *Int J Pharm*. 1993;89(1):R9-R12. doi:10.1016/0378-5173(93)90313-5

16. Cavalli R, Caputo O, Gasco MR. Preparation and characterization of solid lipid nanospheres containing paclitaxel. *Eur J Pharm Sci Off J Eur Fed Pharm Sci*. 2000;10(4):305-309. doi:10.1016/s0928-0987(00)00081-6

17. Martins S, Tho I, Reimold I, et al. Brain delivery of camptothecin by means of solid lipid nanoparticles: Formulation design, in vitro and in vivo studies. *Int J Pharm*. 2012;439(1-2):49-62. doi:10.1016/j.ijpharm.2012.09.054

18. Simovic S, Heard P, Hui H, et al. Dry Hybrid Lipid–Silica Microcapsules Engineered from Submicron Lipid Droplets and Nanoparticles as a Novel Delivery System for Poorly Soluble Drugs. *Mol Pharm*. 2009;6(3):861-872. doi:10.1021/mp900063t

19. Shirodkar RK, Kumar L, Mutalik S, Lewis S. Solid Lipid Nanoparticles and Nanostructured Lipid Carriers: Emerging Lipid Based Drug Delivery Systems. *Pharm Chem J*. 2019;53(5):440-453. doi:10.1007/s11094-019-02017-9

20. Masurier N, Aruta R, Gaumet V, et al. Selective C-Acylation of 2-Aminoimidazo[1,2- *a*]pyridine: Application to the Synthesis of Imidazopyridine-Fused [1,3]Diazepinones. *J Org Chem*. 2012;77(7):3679-3685. doi:10.1021/jo300364d

21. Bandopadhyay S, Bandyopadhyay N, Deb PK, Singh C, Tekade RK. Preformulation Studies of Drug Substances, Protein, and Peptides. In: *Dosage Form Design Considerations*. Elsevier; 2018:401-433. doi:10.1016/B978-0-12-814423-7.00012-5

22. Cheng T, Zhao Y, Li X, et al. Computation of Octanol–Water Partition Coefficients by Guiding an Additive Model with Knowledge. *J Chem Inf Model*. 2007;47(6):2140-2148. doi:10.1021/ci700257y

23. Doufène K, Lapinte V, Gaveau P, et al. Tunable vegetable oil / silica hybrid microparticles for poorly water-soluble drug delivery. *Int J Pharm*. Published online June 2019:118478. doi:10.1016/j.ijpharm.2019.118478

24. Phillips DJ, Pygall SR, Cooper VB, Mann JC. Overcoming sink limitations in dissolution testing: a review of traditional methods and the potential utility of biphasic systems. *J Pharm Pharmacol*. 2012;64(11):1549-1559. doi:10.1111/j.2042-7158.2012.01523.x

25. Phillips DJ, Pygall SR, Cooper VB, Mann JC. Toward Biorelevant Dissolution: Application of a Biphasic Dissolution Model as a Discriminating Tool for HPMC Matrices Containing a Model BCS Class II Drug. *Dissolution Technol*. 2012;19(1):25-34. doi:10.14227/DT190112P25

26. Denninger A, Westedt U, Rosenberg J, Wagner KG. A Rational Design of a Biphasic Dissolution Setup—Modelling of Biorelevant Kinetics for a Ritonavir Hot-Melt Extruded Amorphous Solid Dispersion. *Pharmaceutics*. 2020;12(3):237. doi:10.3390/pharmaceutics12030237

27. Velázquez-Olvera S, Salgado-Zamora H, Velázquez-Ponce M, Campos-Aldrete E, Reyes-Arellano A, Pérez-González C. Fluorescent property of 3-hydroxymethyl imidazo[1,2-a]pyridine and pyrimidine derivatives. *Chem Cent J*. 2012;6(1):83. doi:10.1186/1752-153X-6-83

28. Masurier N, Moreau E, Lartigue C, et al. New Opportunities with the Duff Reaction. *J Org Chem*. 2008;73(15):5989-5992. doi:10.1021/jo800700b

29. Collins DS, Sánchez-Félix M, Badkar AV, Mrsny R. Accelerating the development of novel technologies and tools for the subcutaneous delivery of biotherapeutics. *J Controlled Release*. 2020;321:475-482. doi:10.1016/j.jconrel.2020.02.036

30. Bragta P, Sidhu RK, Jyoti K, et al. Intratumoral administration of carboplatin bearing poly (ε-caprolactone) nanoparticles amalgamated with in situ gel tendered augmented drug delivery, cytotoxicity, and apoptosis in melanoma tumor. *Colloids Surf B Biointerfaces*. 2018;166:339-348. doi:10.1016/j.colsurfb.2018.03.009

31. Golombek SK, May J-N, Theek B, et al. Tumor targeting via EPR: Strategies to enhance patient responses. *Adv Drug Deliv Rev*. 2018;130:17-38. doi:10.1016/j.addr.2018.07.007

32. Hamaguchi T, Matsumura Y, Suzuki M, et al. NK105, a paclitaxel-incorporating micellar nanoparticle formulation, can extend in vivo antitumour activity and reduce the neurotoxicity of paclitaxel. *Br J Cancer*. 2005;92(7):1240-1246. doi:10.1038/sj.bjc.6602479

33. Smylie MG, Wong R, Mihalcioiu C, Lee C, Pouliot J-F. A phase II, open label, monotherapy study of liposomal doxorubicin in patients with metastatic malignant melanoma. *Invest New Drugs*. 2006;25(2):155-159. doi:10.1007/s10637-006-9002-y

34. Wagner S, Rothweiler F, Anhorn MG, et al. Enhanced drug targeting by attachment of an anti αv integrin antibody to doxorubicin loaded human serum albumin nanoparticles. *Biomaterials*. 2010;31(8):2388-2398. doi:10.1016/j.biomaterials.2009.11.093

Figures captions

Scheme 1. Proposed mechanisms for the formation of ORD and ORALD.

Figure 1. Chemical structure of JMV5038 and its open-ring derivative (ORD).

Figure 2. Experimental set-up of the dialysis device within a PBS/octanol biphasic system under magnetic stirring. The system is thermostated at 37 °C.

Figure 3. Thermogravimetric analysis of JMV5038 and its ORD under nitrogen atmosphere.

Figure 4. Differential scanning calorimetry analysis of JMV5038 and its ORD under nitrogen atmosphere.

Figure 5. Optical microscopy observation (on the left) and particle size measurement (on the right) of the HNP suspension. n = 3.

Figure 6. UPLC traces of compounds released from HNP formulated in acidic medium (A) or from HNP formulated in neutral medium (B), compared to pure JMV5038 (D) and ORD (C), at λ = 214 nm.

Figure 7. *In vitro* cumulative release of JMV5038 from HNP in a PBS/octanol biphasic system at 37 °C.

Figure 8. (A) Activity of loaded and unloaded HNP on A375 cells compared to control at four corresponding concentrations. One asterisk and two asterisks correspond to p values < 0.05 and < 0.01, respectively (B) Cell viability dose-response curve of A375 cells treated by JMV5038-loaded or unloaded HNP, JMV5038, or ORD; (C) Calculated IC50. All results are mean ± standard deviation (SD) of three independent experiments.

Figure 9. Cell viability of NIH 3T3 exposed to unloaded or JMV5038-loaded HNP. All results are mean ± SD of three independent experiments, and asterisk corresponds to a p value < 0.05 compared to the control.

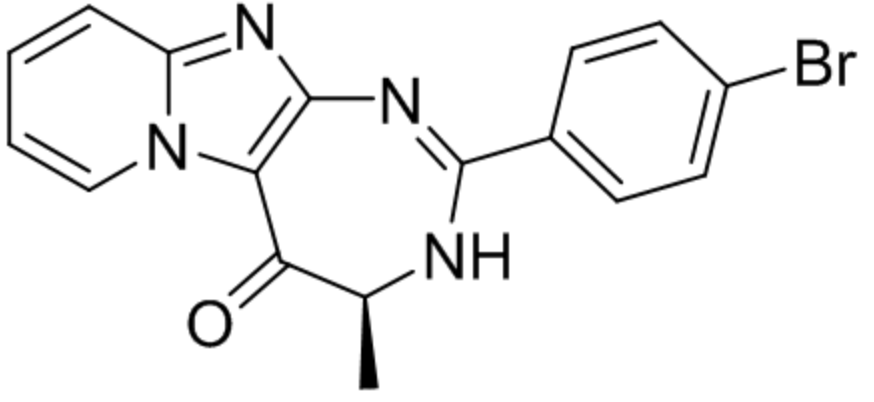

JMV5038

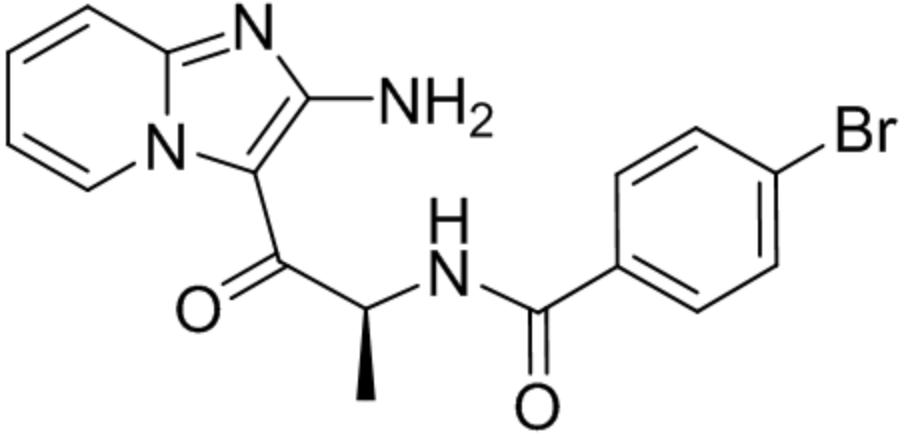

ORD

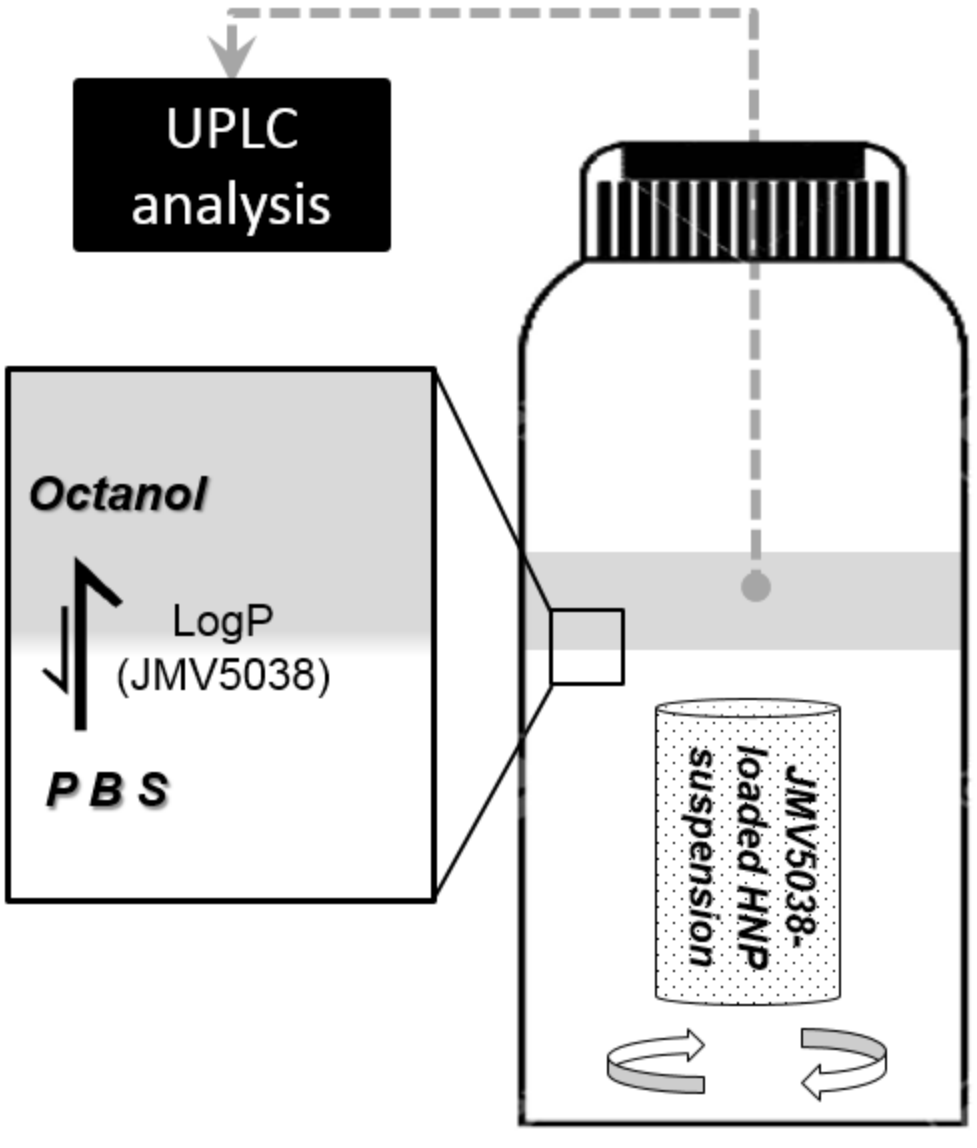
UPLC
analysis
Octanol
LogP
(JMV5038)
PBS
JMV5038-
loaded HNP
suspension

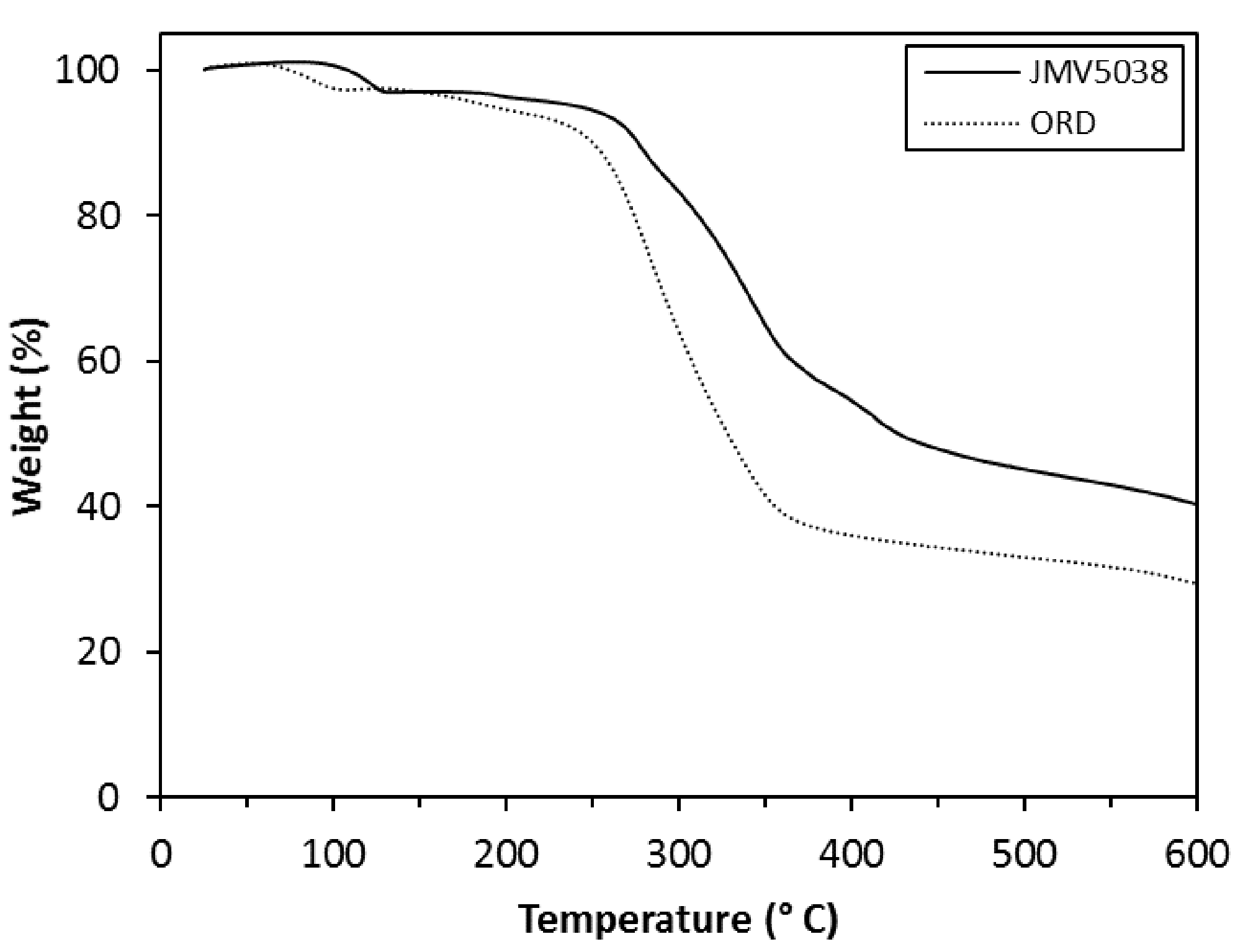
JMV5038
ORD
100
80
60
40
20
0
Weight (%)
0
100
200
300
400
500
600
Temperature (° C)

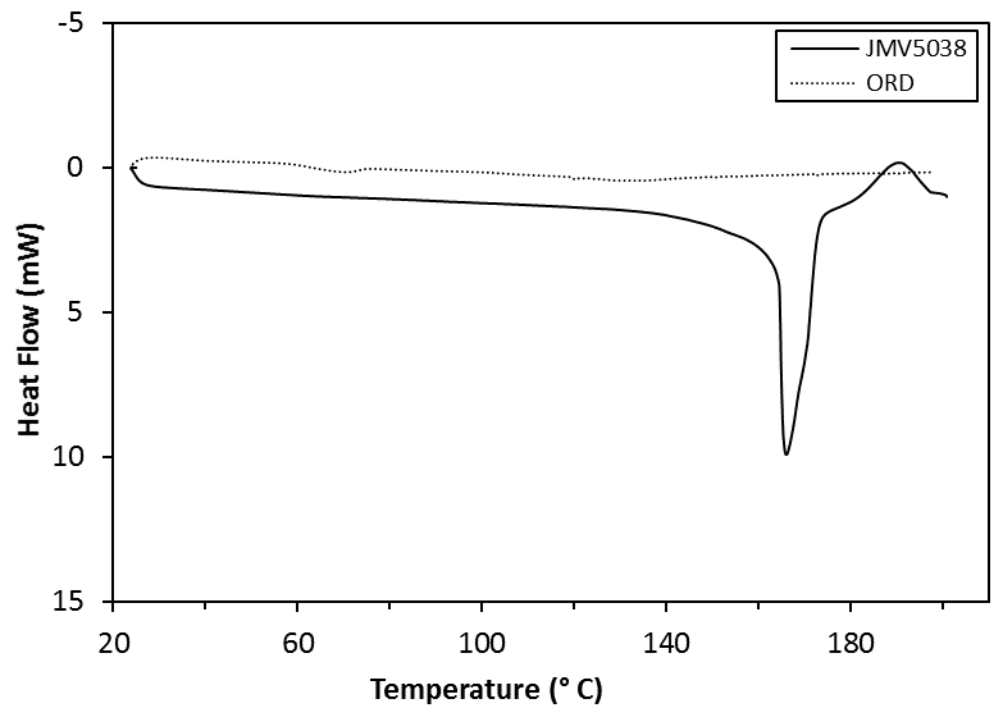
JMV5038
ORD
-5
0
5
10
15
Heat Flow (mW)
20
60
100
140
180
Temperature (° C)

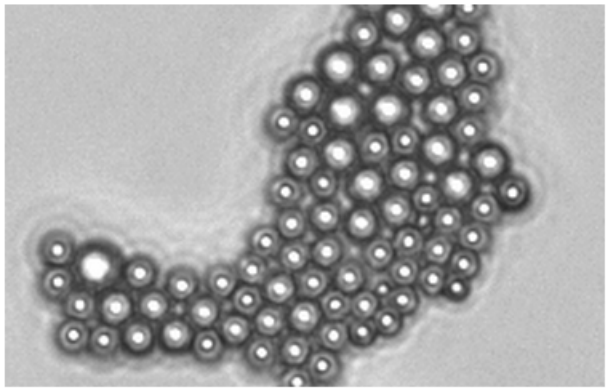

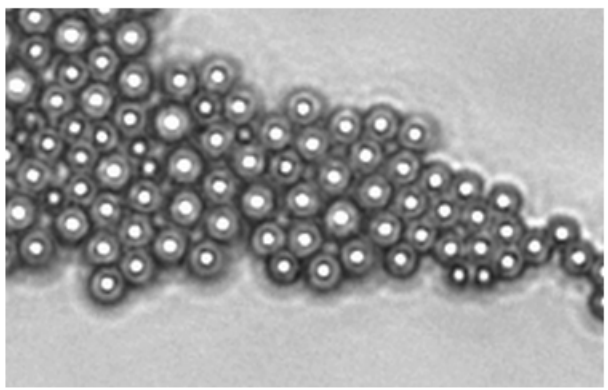

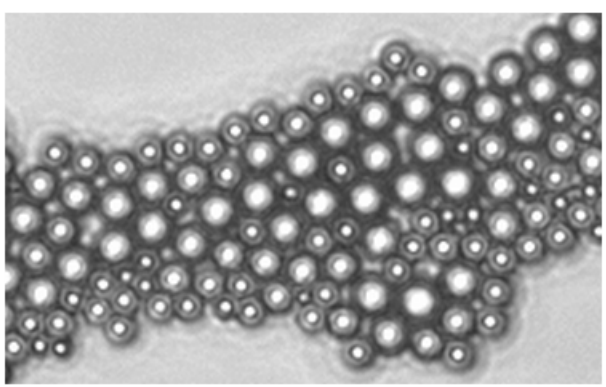

5 µm

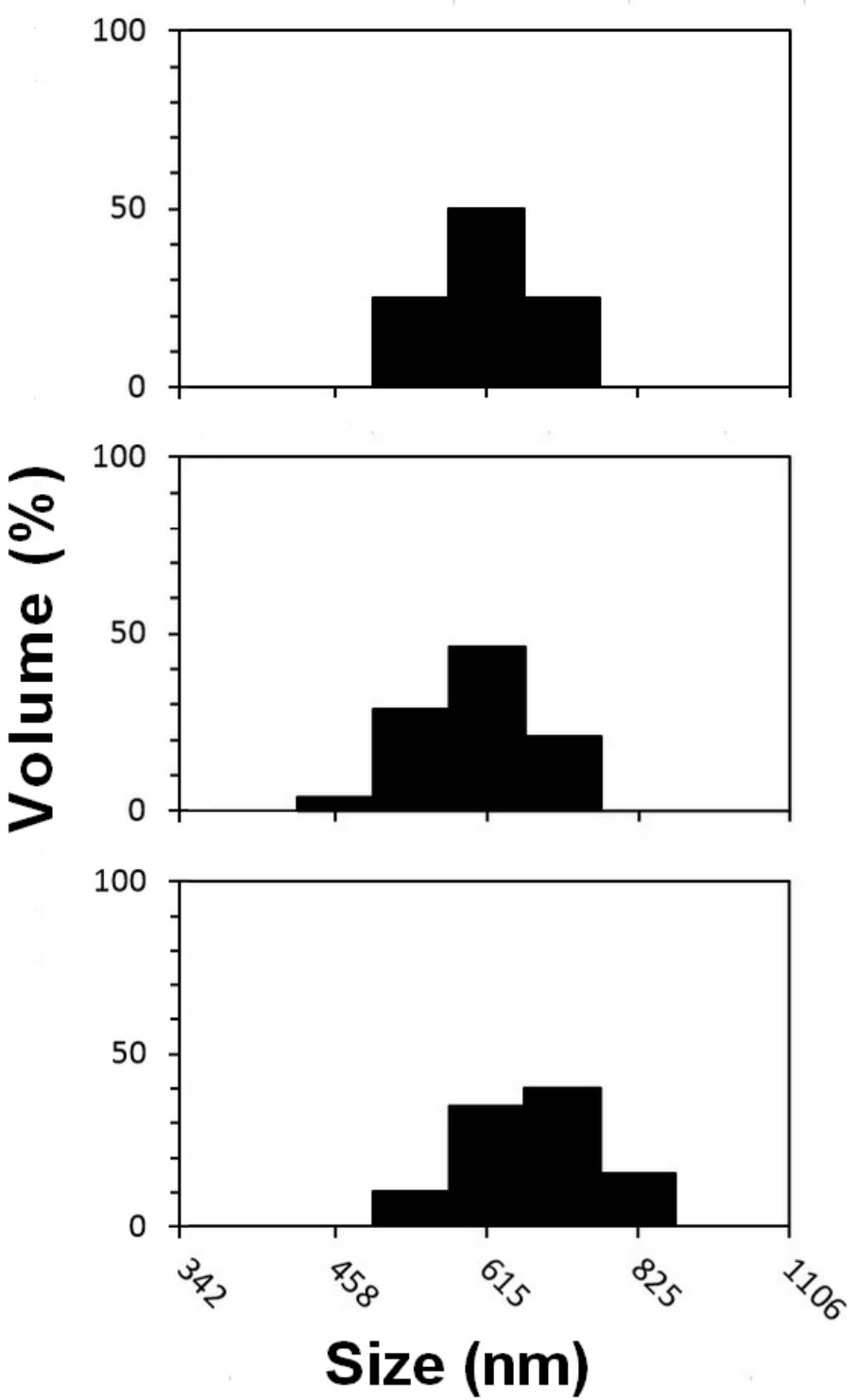

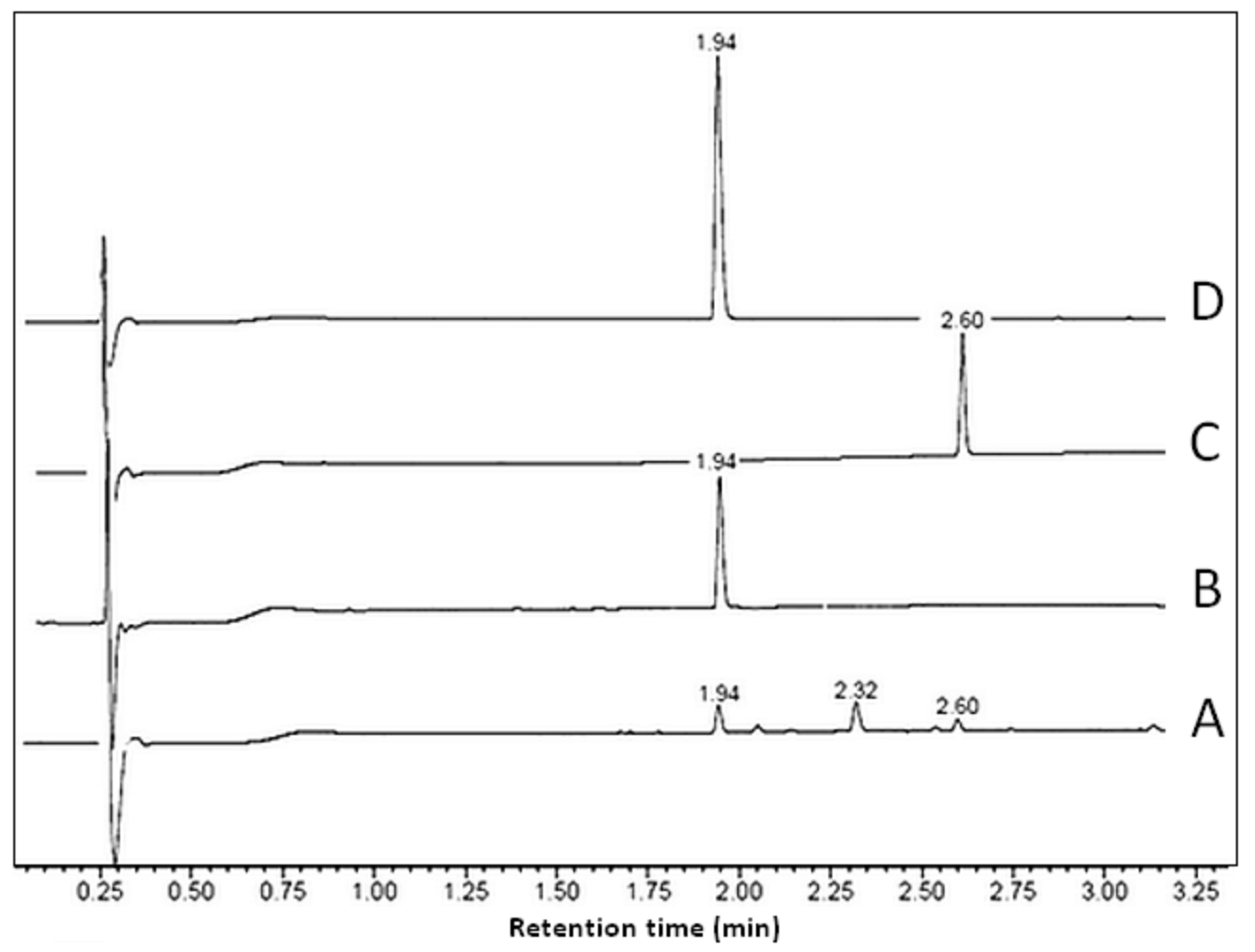
1.94
D
2.60
C
1.94
B
1.94
2.32
2.60
A
0.25
0.50
0.75
1.00
1.25
1.50
1.75
2.00
2.25
2.50
2.75
3.00
3.25
Retention time (min)

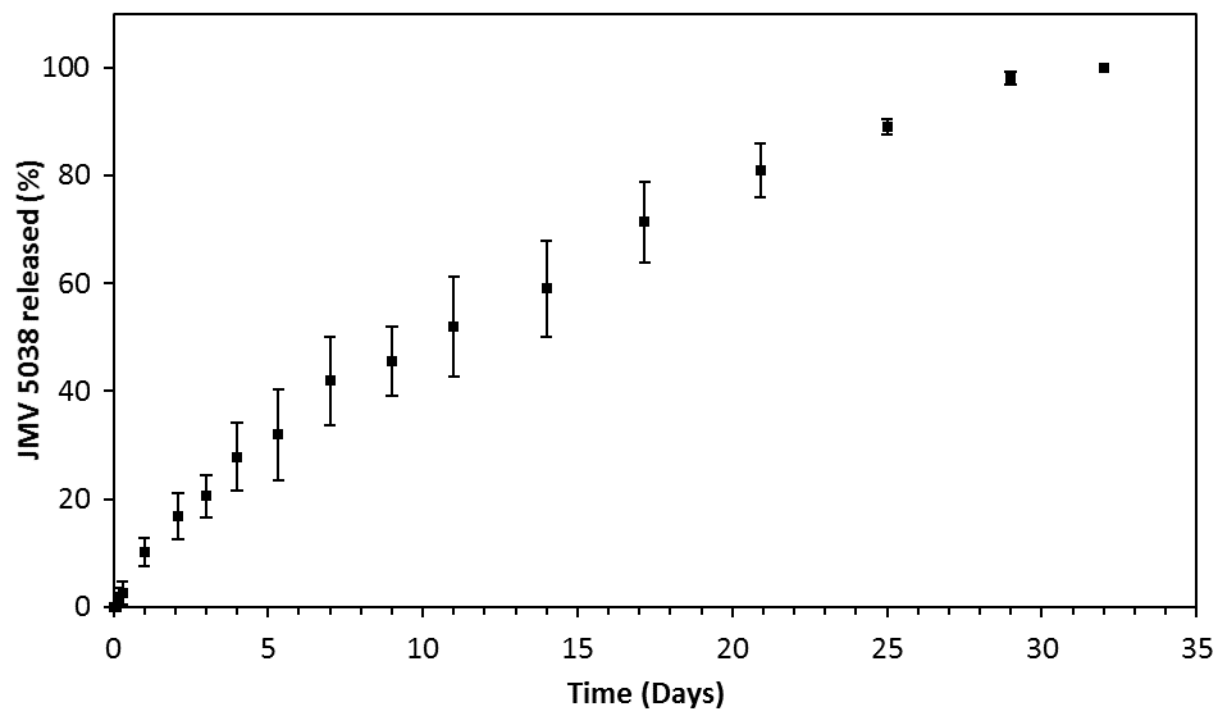
JMV 5038 released (%)
0
20
40
60
80
100
0
5
10
15
20
25
30
35
Time (Days)

A

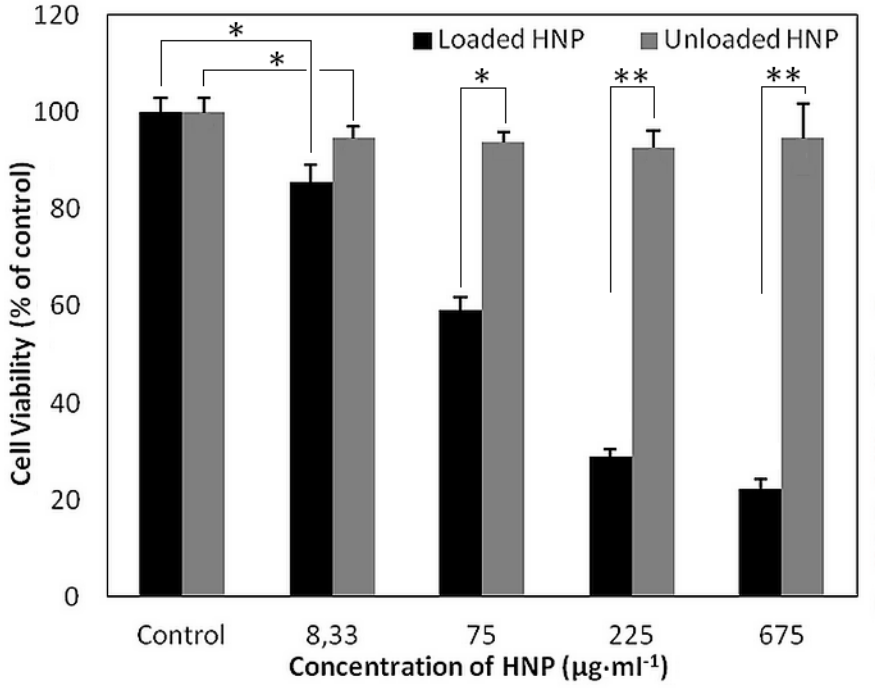

B

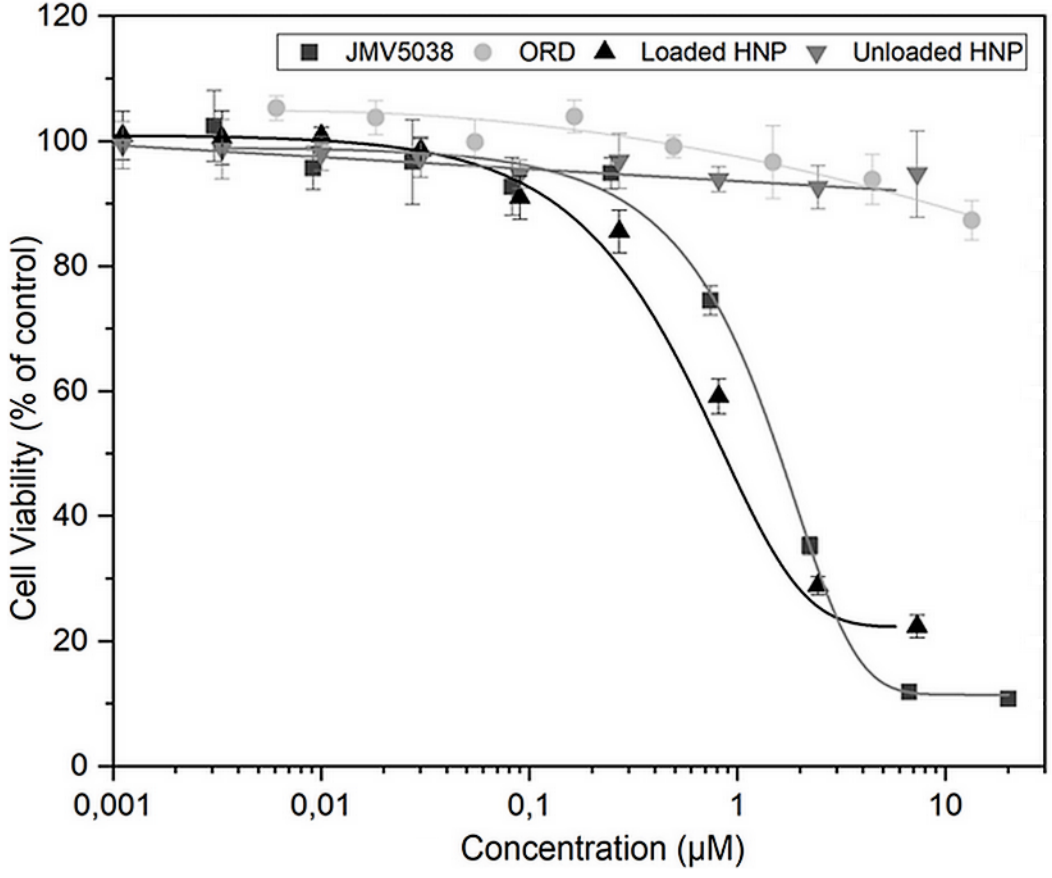

C

	Loaded HNP	Unloaded HNP	JMV5038	ORD
IC_{50} (µM)	1.58 ± 0.03	> 40	2.10 ± 0.42	> 40

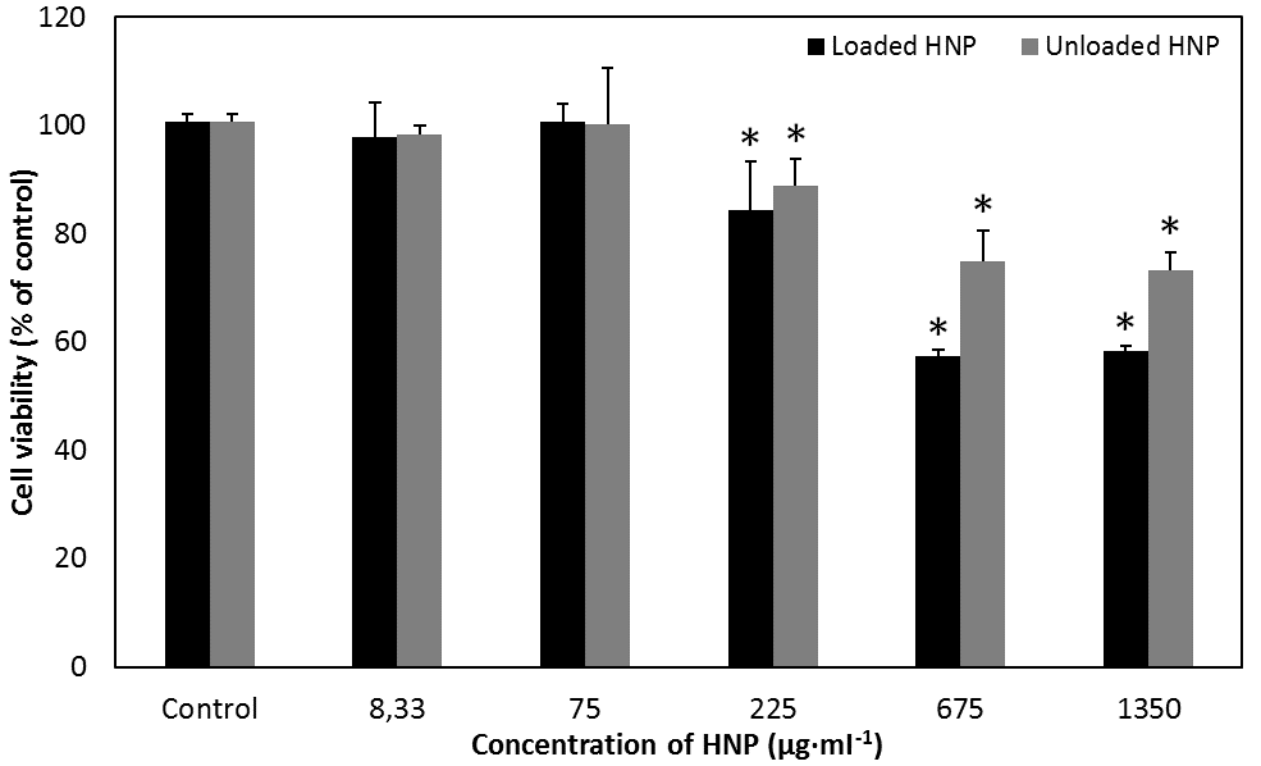
120
100
80
60
40
20
0
Cell viability (% of control)
Loaded HNP
Unloaded HNP
*
Control
8,33
75
225
675
1350
Concentration of HNP (µg·ml-1)